C–8–2

MEASUREMENT OF RAIN ATTENUATION BY DUAL-FREQUENCY RADAR

Matsuichi YAMADA, Akiyoshi OGAWA, Osamu FURUTA and Hiroshi YOKOI
Research and Development Laboratories, Kokusai Denshin Denwa Co., Ltd.
2-1-23, Nakameguro, Meguro-ku, Tokyo 153, Japan

Introduction

Various measurements of rain attenuation by use of meteorological radar have been made over the past years. These methods by conventional radar, however, used to have considerable errors, since they needed to employ an empirical equation relating radar reflectivity to rain attenuation for deriving rain attenuation from the received radar echo.

In order to reduce such errors as mentioned above, the authors have developed a new meteorological radar employing dual frequencies which provides an useful means for measuring rain attenuation at frequencies above 10 GHz. This radar transmits two radiowaves at 5- and 14-GHz bands simultaneously. By comparing received echo powers at both frequency bands, rain attenuation at 14-GHz band can be directly obtained without knowing the value of radar reflectivity.

This paper describes the principle of measurement, the configuration of experiment system and the measurement results, and also presents some discussions on the attenuation measurement using dual-frequency radar system.

2 Principle of measurement

In general, radar equation is expressed by

$$P_r = C\cdot\frac{1}{r^2}\cdot\eta\cdot 10^{-0.2\int_0^r 2(K_A+K_R)dr}, \qquad (1)$$

where
P_r : receiving power of radar
r : distance between radar and scattering volume
η : back-scattering cross section of precipitation particles in unit volume
K_A : one-way attenuation due to atmospheric gases
K_R : one-way attenuation due to rain,
and also C is a constant given by the following equation:

$$C=\frac{P_t\cdot h\cdot G_0^2\cdot\theta_0^2\cdot\lambda^2}{2^{10}\cdot\log_e 2\cdot\pi^2}, \qquad (2)$$

where
P_t : peak power of transmit signal
h : spatial length of transmit pulse
G_0 : antenna gain
θ_0 : half-power-beamwidth of radar antenna
λ : wave length.

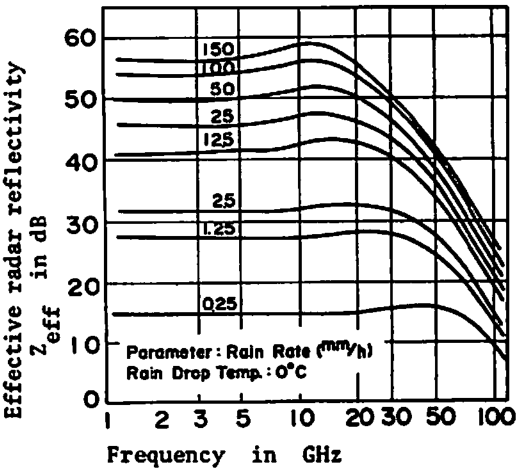

Fig.1 Frequency Dependence of Effective Radar Reflectivity Z_{eff}

Applying Rayleigh's scattering theory, η for conventional radar is denoted by

$$\eta_{\mathrm{Rayleigh}} = \frac{\pi^5}{\lambda^4} \left| \frac{\varepsilon - 1}{\varepsilon + 2} \right|^2 \sum_{a_{\min}}^{a_{\max}} N(a)(2a)^6 \quad , \qquad (3)$$

where ε : complex dielectric constant of rain water
a : radius of raindrop
N(a) : size distribution of raindrop with radius a per unit volume.

The term of $\Sigma N(a)(2a)^6$ in the equation (3) is known as radar reflectivity Z.

However, in case of the dual-frequency radar mentioned here, η_{Mie} given by Mie's scattering theory should be used, since the Rayleigh's approximation is inapplicable at frequencies above 10 GHz. Referring to the equation (3), the effective radar reflectivity Z_{eff} in η_{Mie}, instead of Z in η_{Rayleigh}, can be defined as

$$Z_{\mathrm{eff}} = \eta_{\mathrm{Mie}} \cdot \frac{\lambda^4}{\pi^5} \left| \frac{\varepsilon + 2}{\varepsilon - 1} \right|^2 . \qquad (4)$$

Fig. 1 shows the frequency dependence of Z_{eff}, assuming that the size distribution N(a) of raindrops obeys Laws and Parsons' one. It should be noted in this figure that Z_{eff} has little frequency dependence at frequencies below 20 GHz. Accordingly, from the comparison of received echo powers at 5- and 14-GHz bands, the rain attenuation at 14-GHz band can be determined directly by eliminating the radar reflectivities at both frequencies, since the rain attenuation at 5-GHz band is negligibly small.

3 Configuration of experiment system

Fig.2 is a block diagram of the experiment system installed at Ibaraki Satellite Communication Center of KDD. The antenna used is of Cassegrain type with the aperture of 7 m in diameter. The elevation angle of the antenna has been usually fixed at 10 degrees.

Pulses at 5- and 14-GHz bands, with duration of 1.1 μs, are alternatively emitted from the antenna at every 3 ms. Table 1 shows the performance of dual-frequency radar system.

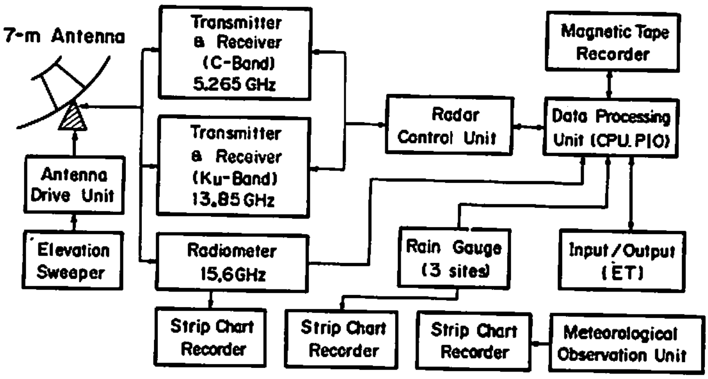

Fig.2 Block Diagram of Experiment System

Peak Transmit Power	50 KW
Pulse Duration	1.1 μs
Pulse Repitition Frequency	163 Hz
IF Band Width	5.5 MHz
Max. Detectable Level	-20 dBm
Min. Detectable Level	5 GHz : -99 dBm 14 GHz : -97 dBm
Resolution of Attenuation	0.3 dB
Resolution of Distance	300 m
Integration Time of Data	2/5/15/30 sec

Table 1 Performance of Dual-Frequency Radar

4 Results of measurement

4.1 Rain attenuation at 14-GHz band

Fig. 3 shows an example of measurement result at the fixed elevation angle of 10° on Dec. 13, 1974. The rain rate at the radar site is about 2 mm/h. It is seen from the figure that received echo power at 14-GHz band decreases with distance more rapidly than that at 5-GHz band. It is attributed to the difference between rain attenuations at the above two frequencies. Since rain attenuation at 5-GHz band can be regarded as negligibly small, the above-mentioned difference is considered to be due to rain attenuation at 14-GHz band. Significant increase of Z around 7-km point from the radar site will be due to the existence of intense rainfall region. As the result, the sudden increase of rain attenuation at 14-GHz band is also seen around this region.

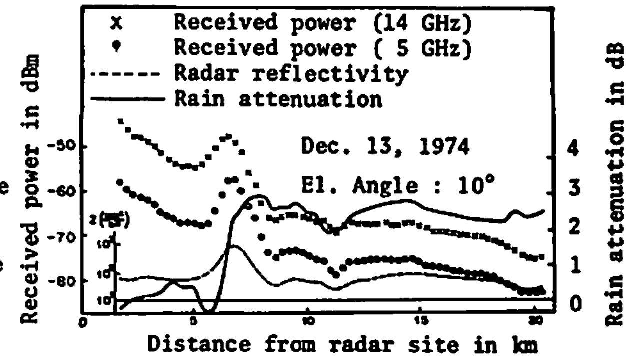

Fig.3 Example of Data

Fig. 4 shows the cummulative time distribution of 14-GHz rain attenuation at the elevation angle of 10° and rain rate for one year from June 1975 to June 1976. The total amount of rainfall during measuring period was 1649 mm. Attenuation values for 0.1 and 0.01% of the time are 13.6 and 26.0 dB, respectively, and also rain rates for the above-mentioned percentages are 19 and 54 mm/h, respectively. In addition, the effective path lengths for rain at 0.1 and 0.01% of the time can be calculated to be 14.5 and 8.7 km, respectively.

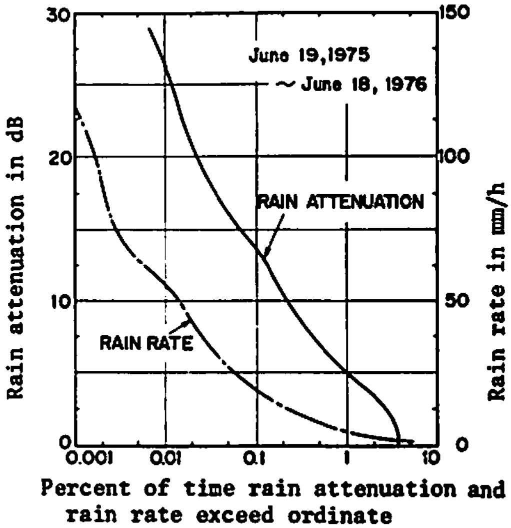

Fig. 4 Cummulative Time Distributions of Rain Attenuation at 14 GHz (El=10°) and Rain Rate

4.2 Vertical structure of rainfall

Fig. 5 shows the yearly cummulative time distribution of radar reflectivity Z, deduced from observation data at 5-GHz band, at various points along the propagation path from the radar site. Since the observation angle is 10° in elevation, the altitude of radar target increases with distance from the radar site. Accordingly, Fig.5 can be said to represent the statistical altitude dependence of radar reflectivity Z. It is known, from the figure, that rain at the altitude below about 3 km has similar statistical properties on drop-size distribution to those at the earth surface. On the other hand, the curves around the altitude of 4 km are supposed to be largely affected by hydrometeors at bright band.

5 Discussion

Dual-frequency radar, as mentioned in the paper, has great advantage that it can derive the spatial structure of rainfall region as well as the characteristics of rain attenuation. However, on the other hand, it has some problems peculiar to radar application.

Fig.6 shows a measurement example in which there is a heavy rainfall region at 3.5-km point from radar site. As is seen in the figure, the gradient of attenuation versus distance is apt to be negative at the rear part of such a heavy rainfall region as Z increases rapidly.

The half-power-beamwidth of the radar antenna had been, at first, about 0.2° and 0.5° at 14- and 5-GHz bands, respectively. In order to examine whether the difference between antenna beamwidths at the two frequencies causes the negative attenuation as mentioned above or not, beam equalization at both frequency bands has been attempted by modifying the sub-reflector surface of the radar antenna. According to the preliminarily analyzed results of data obtained after that, the difference of antenna beamwidth is unlikely to be the decisive reason of such extraordinary phenomenon as shown in Fig.6. Further consideration seems to be needed on physical characteristics of rainfall media, for example, such as frequency dependence of radar reflectivity, the influence of rain depolarization effect and so on.

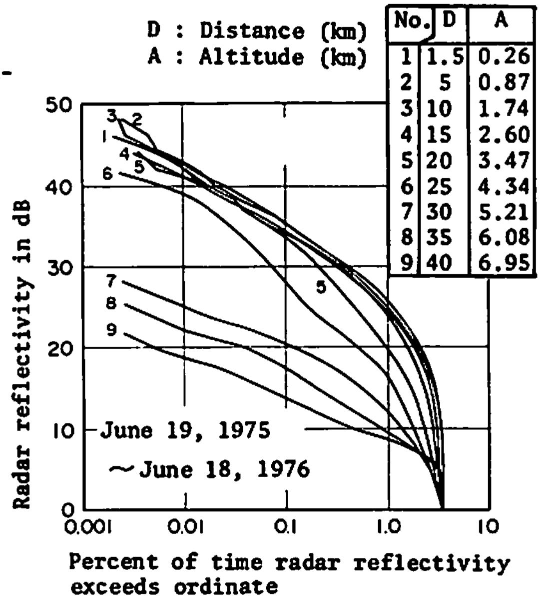

No.	D	A
1	1.5	0.26
2	5	0.87
3	10	1.74
4	15	2.60
5	20	3.47
6	25	4.34
7	30	5.21
8	35	6.08
9	40	6.95

Fig.5 Altitude Dependence of Radar Reflectivity

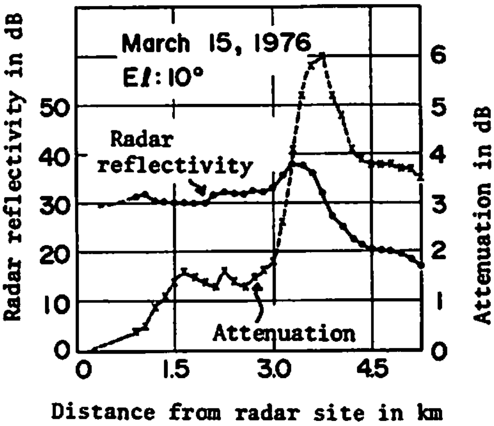

Fig.6 An Example of Receiving Data

Also, on measurement data above bright band, such reverse phenomenon of rain attenuation as shown in Fig.6 has been frequently observed. This might be ascribed to the frequency dependence of reflective characteristics at bright band. However, since the attenuation due to the particles above bright band is generally considered to be small compared to the one due to raindrops, this influence has been ommitted in data analysis.